Heliyon 8 (2022) e12194

Contents lists available at ScienceDirect

Heliyon

journal homepage: www.cell.com/heliyon

Research article

# Modelling of *Lemna minor* L. growth as influenced by nutrient supply, supplemental light, $CO_2$ and harvest intervals for a continuous indoor cultivation

Karl-Michael Schmidt *, Heiner E. Goldbach

*University of Bonn, INRES, Karlrobert-Kreiten-Str. 13, 53115 Bonn, Germany*

## HIGHLIGHTS

· A $NH_4^+/NO_3^-$ ratio of 1:9 at a total N-concentration of 1.14 mM kept pH and growth rates constant.
· The model predicts the optimal harvest point, amounts to be harvested and harvest intervals with high accuracy.
· Maximum yield over time was obtained by cyclic partial harvesting along a sigmoidal growth curve.
· Supplemental $CO_2$ at 3,500 ppm increased growth rate and yield by 44% at a light quantity of 129.44 μmol. $s^{-1}{\cdot}m^{-2}$
· Liebig's law of the minimum, referred to as Blackman limitation, is implicitly part of the developed model.

## ARTICLE INFO

*Keywords:*
Lemnaceae
Lndoor-cultivation
Carbon dioxide $CO_2$
Nutrient medium
Specific PAR spectra
Modelling
Michaelis-Menten
Yield
Biomass production
Liebig's law of the minimum

## ABSTRACT

Given the proper conditions, *Lemna spp.* rapidly produce a high amount of valuable biomass which is considered as an alternative source for feed and food. For a continuous and long-term indoor production under controlled conditions, environmental and harvest parameters have to be optimized to suppress algal growth and constantly yield a high-quality product. Experimentally assessing the effect of a larger number of parameters on the growth rate $r_i$ is impossible due to the theoretically high number of parameter combinations. Thus, a SIMILE® - based model has been developed. This enables production parameters to be assessed individually for its effect on the growth rate $r_i$ by a differential equation. Start values for numerical integration were taken from measured data and analytical solutions of the differential growth equation. At 400 ppm $CO_2$, the regrowth rate *ri* in an optimized laboratory set-up amounted to 216 g $FM{\cdot}m^{-2}d^{-1}$, harvesting one third of the biomass at intervals of 5 days. In up-scaled set-ups, lower regrowth rates *ri* of about 173 g $FM{\cdot}m^{-2}d^{-1}$ (Kalkar) and 190 g $FM{\cdot}m^{-2}d^{-1}$ (Berlin) were obtained, because temperature and light conditions were below optimum. At 3,500 ppm $CO_2$, the regrowth rate *ri* in laboratory set-up increased to 323 g $FM{\cdot}m^{-2}d^{-1}$ by shortening the harvest interval to three days. Maximum growth rates *ri* were obtained with an $NH_4^+/NO_3^-$ ratio of 1/9 at 1.14 mM total N concentration. The results indicate how to optimize culture conditions and harvest intervals. Model runs closely match the experimental data taken from the three different approaches and thus confirm the validity of the model.

## 1. Introduction

### 1.1. Nutritional value

*Lemnoideae* are considered as a valuable nutrient source, (Appenroth et al., 2017; Chakrabarty et al., 2018), for an increasing protein demand. In addition, they are rich in poly-unsaturated fatty acids (PUFA) (Landolt, Kandeler 1987; Kuehdorf, Appenroth 2012). The world health organization (WHO) recommended this biomass according to its nutritional value as "novel food" (Calabrese, Ferranti 2019). Because of the rapid growth by clonal propagation and facile uptake from media were attractive features *Lemnoideae* were well known model plant for plant biology between 1950 and 1990 (Acosta et al., 2021).

### 1.2. Controlled indoor cultivation

The authors have developed an indoor system for year-round growth of *Lemna spp.* As a source for novel food and further substances (Schmidt

* Corresponding author.
*E-mail address:* karl-michael.schmidt@gmx.de (K.-M. Schmidt).

https://doi.org/10.1016/j.heliyon.2022.e12194
Received 21 July 2022; Received in revised form 20 October 2022; Accepted 30 November 2022

2020, 2021; Schmidt et al., 2018). To this end, growth parameters have to be optimized to provide a continuous uninhibited growth and constant quality (Petersen et al., 2022) Given the numerous possible combinations of e.g. temperature, nutrient concentrations and ratios, light, $CO_2$ levels and harvest schedules, a model approach had to be developed where the best combination of many factors can be assessed. In order to assure hygienic requirements for the final product, a protected indoor production with standardized conditions is the method of choice (Coughlan et al., 2022). A large – scale cultivation can only be non-axenic to keep costs at bay. Under the respective conditions, Petersen et al. (2021) achieved a relative growth rate (RGR) for the dry matter of *Lemna minor* of about 0,23 ± 0,009 $d^{-1}$. Their cultivation period lasted, however, only 7 days. A constant long-term production faces the problem of a competitive algal growth (Ueda, Nagai 2021) which may completely spoil the biomass for its use as novel food (Szabo et al., 2005). Competition by algal growth was hardly ever observed in short term experiments under non-axenic conditions, but is a severe thread for long-term cultivation. This can be influenced to a large extend by the $NH_4^+/NO_3^-$ ratios in the nutrient solution. Khvatkov et al. (2019) used a modified Hoagland and Arnon solution (Hoagland, Arnon 1938) and measured various $NH_4^+/NO_3^-$ ratios in relation to the resulting growth rates, where a ratio ≤1/13 was found as optimum under axenic conditions and with only 65 µmol $s^{-1}{\cdot}m^{-2}$ supplemental light. Considering the dynamics of $NO_3^-$ and $NH_4^+$ uptake in duckweed (Zhou et al., 2021), a $NH_4^+/NO_3^-$ ratio of 25/75, as used by Petersen et al. (2021, 2022), cannot be confirmed as appropriate under conditions of long term cultivation. According to light adaption, circadian clock effects have to be considered (Ueno et al., 2021) by taking care of 16/8 (light/dark) photoperiods in all experiments at all locations.

### 1.3. Model approach

As there is yet a lack of in depth long-term studies for continuous *Lemna* cultivation, the authors started an approach, where the most important cultivation factors including harvest intervals and nutrient supply were assessed as outlined below:

i) the optimum growth medium regarding nutrient supply rates and ratios (Lasfar et al., 2007),

ii) optimum supplemental light in quantity and quality (Petersen et al., 2022; Stewart et al., 2020)

iii) optimum temperature (Farquhar, von Caemmerer 1982; von Caemmerer, Farquhar 1981)

iv) supplemental $CO_2$ (Raven et al., 1985) as related to the available photosynthetically active radiation (PAR). An already existing model approach (Khvatkov et al., 2018; Lasfar et al., 2007; van Dyck et al., 2022) had to be refined further. In addition, the influence of periodic harvesting of the existing *Lemna* biomass had to be considered as it influences coverage and competition by algae. Driever et al. (2005) indicated that *Lemna* populations grow until reaching defined limits. It has to be taken into account that the *Lemna* fronds form a compact layer on the water surface, finally limiting its further growth (competition for light, nutrients and possibly $CO_2$). Considering Driever's (2005) observations, a strong dependency between partial harvesting, influencing the population density and regrowth rates can thus be expected. So, one has to consider harvested amounts and harvesting intervals, together with the parameters under i) – iv) in the model approach. Below, the authors will present at first the experimental results, especially for an optimized nutrition and harvest intervals, which then will be fed into a model and verified in upscaled systems. Well established concepts of Liebig's law of the minimum (Warsi, Dykhuizen 2017; Morris, Blackwood 2007; Litchman 2007; Smith, Schindler 2009), also referred to as Blackman limitation (Soong et al., 2020) needed to be implemented into a consistent modelling of growth and optimized harvesting method. It was the aim to obtain a cultivation system with constant long-term stabile yields.

## 2. Materials and methods

### 2.1. Experimental set ups

The authors performed the experiments in three systems at different scales, from a fully controlled laboratory system to upscaled technicum systems as described below. The species used in our experiments were *Lemna minor* L., varieties 'Henry DaCapo' EU, CPVO2010/0855, and 'Henry Vitesse' EU, CPVO2010/0854, registered at the CPVO (**C**ommunity **P**lant **V**ariety **O**ffice).

#### 2.1.1. Laboratory setup in Bonn

The laboratory setup at the University of Bonn, as shown in Figure 1, consists of an open-top grow-box installed in an arrangement of two light tables (RHENAC, GreenTec AG, Mobile LED-RACK, product line R-MU) with adjustable wavelengths at 400nm, 440nm, 660nm, 730nm and with additional 3,000K white-light emitters. The surface of the aquatic culture in each tray (borosilicate glass) in this laboratory setup measures 0.018 $m^2$. A number of 24 glass trays was installed, allowing a simultaneous measurement of maximum 6 treatments with 4 replicates, each. The nutrient solution was introduced into each culture tray with a high-precision peristaltic pump array modified from a Skalar analytical continuous flow-analyzer.

A sandwich heating installation of two heater levels, as shown in Figure 1, is controlled separately. The sandwich heating consisted of an air convection heater combined with a conduction heater in sandwich construction. The LED array was controlled for both light tables with a coupled hierarchical primary and secondary computer controller. For introduction of additional $CO_2$ at an average level of 3,500 ppm, the setup was provided with two diffusors with a common feedback controller system, including flux-controller and $CO_2$ sensor.

The amount of PAR light totaled 129.44 µmol $s^{-1}{\cdot}m^{-2}$ (Photon flux density). Light spectra and photon flux densities were similar in all setups. $CO_2$ was supplied using a controlled discontinuous gas injection system by HTK-Hamburg SCENTY® with a MAPAX® control flow box at an average point of around 3,500ppm inside the open-top growth box. Gas purity was 5.0 (99.9990%). Nutrient solutions used in the laboratory setup were both based on the same used salts and concentrations for macro-as well as for micronutrients. In the upscaled setup in Berlin, N and P were supplied from pre-treated nitrified fish sewage. The nutrient solution was then completed by adding salts to the same concentrations and ratios as used in the laboratory setup in Bonn and the upscaled setup at Kalkar.

Specific LED emitters for PAR illumination at 400nm, 440nm, 660nm and 730nm, additionally to a white light emitter at 3,000 K, represented by the spectral distribution between 480nm and 630nm. The used LED installations at the upscaled set ups in Kalkar and at ECF Farmsystems in Berlin possess a similar spectral distribution in quality and quantity.

#### 2.1.2. Upscaled setup in Kalkar

The trays in the stacked system of both upscaled setups, Kalkar and Berlin, were divided into a highly illuminated maturation zone at 129 µmol $s^{-1}{\cdot}m^{-2}$ PAR and a weakly illuminated sprouting zone at 10–17 µmol $s^{-1}{\cdot}m^{-2}$ PAR. Each culture tray in the setup in Kalkar measured 27 m in length and 0.8 m in width. They were divided into three continuous 9 m long zones. As sprouting and chloroplast formation is stimulated under low light conditions, two thirds of the trays only received diffuse residual light of the greenhouse, whereas the last zone was illuminated with LED by NetLed, (Pirkkala, Finland). The illuminated third "maturation zone" serves to finally boost growth and produce the harvestable biomass.

#### 2.1.3. Upscaled setup in Berlin

In the setup at Berlin, the authors also used a stacked culture system of about 20 $m^2$ aquatic surface, installed at an indoor fish-farming

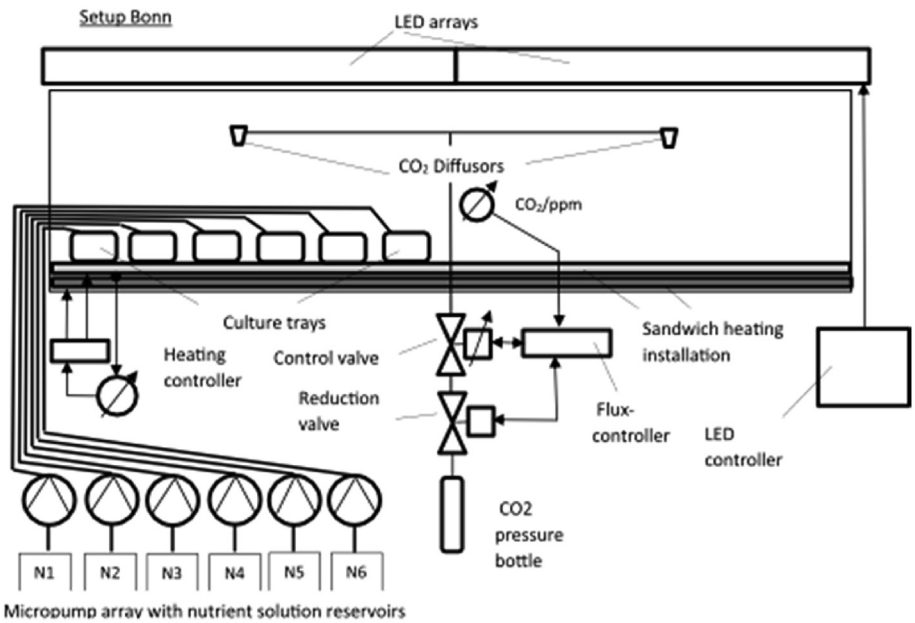


**Figure 1.** Scheme of the grow-box with nutrient dosage system, $CO_2$ supply, heating and LED installation. Nutrient stock solution tanks are provided with an array of peristaltic micropumps. Each pump symbol represents a further array of 4 micropumps for every 4 replicates related to each stock solution; in sum 24 micropumps, which feed 24 culture trays. The micropumps were calibrated *via* a controller and the nutrient solutions were automatically supplied from stock solutions N1–N6 two or three times a day during illumination.

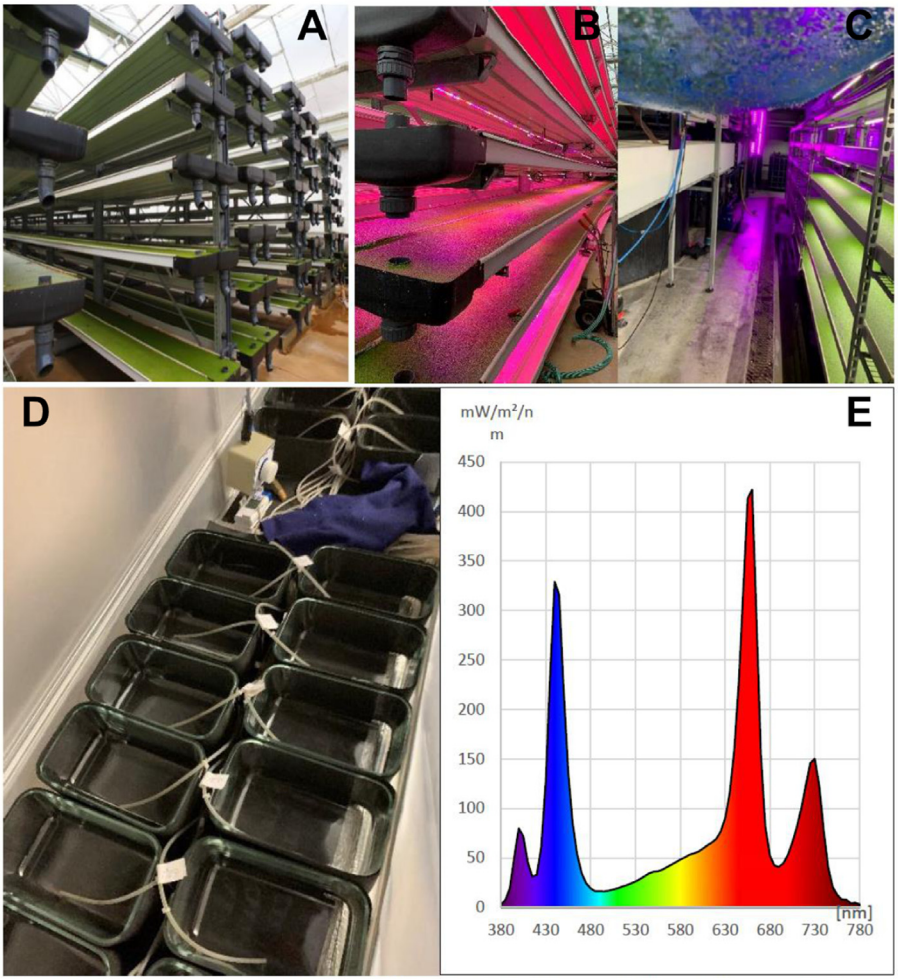


**Figure 2.** (**A**) technicum scale set-ups at Kalkar with 302 $m^2$ aquatic culture surface showing the stacked system at the low lighted sprouting zone and in Figure 2(**B**) the LED illuminated maturation zone. Figure 2(**C**) shows the second upscaled stacked cultivation system with 20$m^2$ aquatic culture surface at ECF Farmsystems in Berlin. Figure 2(**D**) shows a top view into the open-top growth box from the laboratory setup in Bonn, displaying the culture trays with their related nutrient stock solution feed-in tubes, connected to the micro pump array and the related stock solution tanks. Figure (2**E**) shows the computer adjusted spectrum of the supplied LED lighting at the laboratory setup in Bonn.

station. The length of the trays was 9.4 m, as well divided into three thirds as described above: 2/3 of the length as sprouting zone, and 1/3 as LED illuminated maturation zone. Wastewater from the fish farming was used as base of a nutrient solution for the *Lemna* cultures. The fish manure was used after filtering, ozonation, mineralization and nitrification with *Nitrosomonas spp.*, inoculated on micro-structured carriers in

a trickle filter, and adjusted to the same nutrient concentrations and element ratios as in Bonn and Kalkar by adding the respective salts (purity ≥99%, p.a., ACS). Light conditions for sprouting and maturation zone were equal to the setup at Kalkar. The nutrient solutions at all three places were adjusted to the same nutrient ratios and concentrations equal to the optimum found in the lab system at Bonn. The same applies to the supplemental illumination. Therefore, the modelling was carried out for the harvesting conditions in the fully illuminated zone.

### 2.2. Optimizing the nutrient solution

In order to provide a base for the model parameters, the authors first had to optimize nutrient supply (concentration and nutrient ratios), $CO_2$ concentration and temperature. The latter was taken from literature data (Landolt et al., 1987; Docauer, 1983) and has been verified in our own pre-runs to be 29 °C. The concentration ratio between $NH_4^+$ and $NO_3^-$ can be relevant for a species which prefers nitrate over ammonium. The laboratory setup in Bonn served to find the optimum nutrient concentrations and ratios. Each experimental treatment was performed with 4 replicates. Statistics were calculated with MS Excel® software.

In the laboratory setup at Bonn and in the upscaled setup at Kalkar, nutrient salts (p.a. grade) were used to make up the nutrient solutions. The nutrient supply was based on nutrient contents of the biomass, growth rates and the water loss by evapotranspiration, resulting in a modified Hoagland nutrient solution, where $NH_4^+$ was added as $(NH_4)_2SO_4$. Micronutrients supplied as $H_3BO_3$, $MnCl_2{\cdot}4H_2O$, $ZnSO_4{\cdot}7H_2O$, $CuSO_4{\cdot}5H_2O$, and $Na_2MoO_4{\cdot}2H_2O$. Mg was added as $MgSO_4{\cdot}7H_2O$, $Ca^{2+}$ and $NO_3^-$ as $Ca(NO_3)_2{\cdot}4H_2O$, Fe as Fe-EDDHA (Sequestrene®).

The target values for the nutrient solutions at all three sites were as follows: NH $4^+/NO_3^-$ = 1/9, $NH_4^+$ 0.113mM, $NO_3^-$ 1.027mM, $KH_2PO_4$ 0.24mM, Mg 0.4mM, Ca 0.514 mM, Fe 18μM, B 46μM, Mn 9.1μM, Zn 0.77μM, Cu 0.32μM, Mo 0.49μM.

Growth was measured at the points 2 to 5 and 2 to 7 of Figure 4(**A**), (**B**) (below), where the complete population was taken out of the tray using a sterilized medical mesh (polypropylene, 1/3 mm thickness and 1 mm strand spacing, Diversified Biotech®), pushed deeply under the *Lemna* culture and lifted carefully up. The harvested biomass was blotted dry on 8 layers of paper tissue before weighing. Subsequently, the culture was transferred back into the culture tray, the mesh was removed, taking care not to damage the sensitive roots.

### 2.3. Model development

#### 2.3.1. Basic differential equation

A differential equation for limited growth is the basis for our growth model.

$$\frac{dW(t)}{dt} = ri * W \setminus (t) * \left(1 - \frac{W(t)}{Wmax}\right) \quad \text{eq. 1}$$

with.

*W(t)* time dependent development of the population

*ri* growth rate in $g{\cdot}m^{-2}{\cdot}d^{-1}$

$W_{max}$ Capacity, maximum biomass coverage (population density) in $g{\cdot}m^{-2}$ and with implemented term $ri*\frac{W(t)}{Wmax}$

$W_{max}$ in Eq. (1) is the maximum biomass coverage of a specific population, the so-called capacity, which in *Lemnoideae* differs between species and even between cultivars/lines. Because of the high number of individuals per area, the growth of biomass develops with the same mathematical dynamic as the population. Integrating the differential equation Eq. (1), the analytical solution can be described as

$$W(t) = \frac{Wmax}{2} * \left(tanh\left(\frac{ri}{2} * t + \frac{Wmax}{2} * C\right) + 1\right) \quad \text{eq. 2}$$

with the tangens hyperbolicus (tanh) as a specific e-function

$$\tanh = \frac{sinh}{cosh} = \frac{e^x - e^{-x}}{e^x + e^{-x}}$$

The exponent x relates in Eq. (2) to

$$x = \left(\frac{ri}{2} * t + \frac{Wmax}{2} * C\right)$$

The specific constant factor C results from the so-called self-consistent mathematical solution of integration. The exponent *(x)* as such consists of a time-dependent term *(ri/2)* ·*t* and a further term *($W_{max}$/2)* ·*C* which is independent from time. Nevertheless, this integration factor C occurs as a product to be multiplied by $W_{max}$ in the exponential term of the e-function "tanh (tan hyperbolicus)". This strongly indicates that *C* can be interpreted and/or predicted as a species- and/or variety-dependent co-factor to be considered in the growth process of the population. It is supported by the observation over three years of experiments that each variety results in a different capacity $W_{max}$ of the population under the same experimental conditions (light quality and quantity, nutrients, temperature, $CO_2$). For that reason, in the literature, the growth rates are in general indicated for a specific species, (Khvatkov et al., 2018; asfar et al., 2007; Petersen et al., 2021; Petersen et al., 2022; van Dyck et al., 2022). As can be seen below, $W_{max}$ has to be inserted into the model as one of the most important parameters. Moreover, it is possible to identify several species in "reverse-modelling" after a series of comparisons of modelling curves by applying Eq. (2) if the equation is solved towards *C*.

#### 2.3.2. Specification of all growth parameters

As the growth rate *ri* further depends on temperature (T) and photon flux density (E), a modified van't Hoff-Arrhenius relationship by Lasfar et al. (2007) can be used:

$$ri(T) \propto T * \theta 1^{\left(\frac{T-Top}{Top}\right)^2} * \theta 2^{\left(\frac{T-Top}{Top}\right)} \quad \text{eq. 3}$$

$$ri(E) \propto E * \theta 3^{\left(\frac{E-Eop}{Eop}\right)^2} * \theta 4^{\left(\frac{E-Eop}{Eop}\right)} \quad \text{eq. 4}$$

with.

T Temperature.

$T_{op}$ Optimal temperature.

*E* Photonic energy.

$E_{op}$ Optimal photonic energy.

The exponents of the temperature-related *Θ1* and *Θ2* functionals and the radiation-related *Θ3* and *Θ4* become zero when the temperature *T* is permanently kept at $T = T_{op}$ ($T_{op}$ = optimum temperature) and PAR $E = E_{op}$ ($E_{op}$ = optimum light). Therefore, near the respective optima, the values for the functionals*Θi* are 1. Therefore, under these conditions, eq. 3 and eq. 4 are accurately reduced to be linear dependent simply

$$ri(T) \propto T \quad \text{eq. 5}$$

$$ri(E) \propto E \quad \text{eq. 6}$$

Thus, the modelling for a controlled indoor system becomes easy in T and E because of a linear dependency, as resulted in eq. 5 and eq. 6, if in the range near the optimum. The factors for T and E in the optimum can be set to 1, provided that T could be experimentally determined, and to lower than 1 if the system is not operated at the optimum.

The influence of nutrients on the growth rate was taken as described by Driever et al. (2005) and followed Michaelis Menten kinetics.

$$ri(P,N) = \alpha_{P,N} * \frac{C_P}{(C_P + K_P)} * \frac{K_{IP}}{(K_{IP} + C_P)} * \frac{C_N}{(C_N + K_N)} * \frac{K_{IN}}{(K_{IN} + C_N)} \quad \text{eq. 7}$$

with.

$\alpha_{P,N}$ intrinsic growth rate.

$C_P$ P concentration.

$C_N$ N concentration.

$K_{IP}$, $K_P$, $K_N$, $K_{IN}$ constants for saturation and inhibition of P and N.where.

$K_{IP}$ = 101 mg-P/l.

$K_P$ = 0.31 mg-P/l.

$K_N$ = 0.95 mg-N/l.

$K_{IN}$ = 604 mg-N/l.Using Eq. (7) with the aforesaid 1.14 mM-N/l (15.96 mg-N/l) and 0.23 mM-P/l (7,1 mg-P/l), the growth rates for the nutrients N and P result in $r_i(P,N) = \alpha_{(P,N)} \cdot \mathbf{0,98}$. With these levels of N and P, 98% of the possible maximum nutrient related growth rate can be obtained. In consideration of all aforementioned dependencies of the growth rate, $r_i$ results in a so-called product rule, which means, that all influences of temperature, photonic energy, N/P ratio and $CO_2$ being essential, independent from each other and not replaceable, as valid as described by Liebig's law of the minimum,

$$ri = ri0^{*}|\alpha(ri(T))|^{*}|\beta(ri(E))|^{*}|\gamma(ri(N,P))|^{*}|\delta(ri(CO2))| \quad \text{eq. 8}$$

with *ri0* possible maximum growth rate

$\alpha(ri(T))$ α-factor, contribution of temperature to the growth rate

$\beta(ri(E))$ β-factor, contribution of photonic energy to the growth rate

$\gamma(ri(N,P))$ γ-factor, contribution of nutrient ratios to the growth rate

$\delta(ri(CO_2))$ δ-factor, contribution of $CO_2$ concentration to the growth rate.

The multiplication of each related a.m. factor with the maximum possible growth-rate results in the specific growth-rate contribution, and is termed productivity factor *pf*.

The factors $\alpha, \beta, \gamma, \delta$ are each = 1 at the optimum supply and <1 outside of it. This can be used with the cumulation rule (product rule) for the effective growth rate *ri* in the subsequent modelling. Each resulting factor for the parameters temperature, $CO_2$, nutrition and light, is essential for the growth rate and cannot be replaced or compensated by another. The aim of all these factors is, to adjust them in the cultivation as near as possible to 1.0. As seen above, the factor for nutrition for example could be adjusted with 0.98 very near to 1.0, using Eq. (7). Importantly the result from the product rule of Eq. (8), considering the findings of optimization only as being 0.9 for each parameter, this would result in only $0.9^4 = 0.66$ (66%) use of the possible maximum growth potential. This clear indicates how important the optimization of each culture parameter is for a continuous maximal yield and the accuracy of the model.

Further $CO_2$ exposure is significantly effective for an optimal long-term production of *Lemnoideae*. For modelling, the total mesophyll resistance remains the only important factor. Fick's law can be used considering influence of the partial pressure of $CO_2$ for diffusion, (Hikosaka et al., 2015). Thus, the complete further passage of $CO_2$ can be considered as total mesophyll resistance, (Evans et al., 2009). It is important to consider that the guard cells of Lemnoideae keep the stomata constantly opened in adult fronds (Landolt et al., 1987). Thus, this important part of the $CO_2$ pathway remains constant, too. Under the constant conditions of our culture system, this value can be considered as constant near the optimum as well and thus simplified. This results in the definition of a coefficient factor for $r_i(CO_2)$ which can be determined with high accuracy by measuring, and refed as valid value into the model as the aforesaid product rule for the overall growth rate *ri*. In an abbreviated mathematical notation this is

$$< explanationstart > ri = ri0\left(\prod_{j=T,E,NP,CO2} k(ri(j))\right) \quad \text{eq. 9}$$

with k = $\alpha, \beta, \gamma, \delta$ as specific constants.

As a result, the specified new growth formula of Eqs. (2), (8), and (9) results in

$$W(t) = \frac{Wmax}{2}*\left(tanh\left(\frac{ri0}{2}*\left(\prod_{T,E,N,P,CO2} k*ri(j)\right)*t + \frac{Wmax}{2}*C\right) + 1\right) \quad \text{eq. 10}$$

Importantly, we receive a time-dependent exponent

$$\frac{ri0}{2}*\left(\prod_{T,E,N,P,CO2} k*ri(j)\right)*t$$

and the aforementioned time-independent exponent

$$\frac{Wmax}{2}*C$$

The introduction of the term for *ri* into Eq. (2) summarizes all relevant growth factors.

### 2.3.3. Analytical solution

In order to obtain the extrema of the maximal possible harvest amplitude (harvest amount), keeping within the area of quasi-exponential growth of the sigmoidal growth curve W(t), the analytical solution can provide these values by analytical curve discussion.

According to Figure 3, the area of quasi-linear growth extends between the maxima of second derivation and/or zero points of the third derivation. An important conclusive outcome is that the maximal harvest amplitude (amount of cyclic harvest from the culture), indicated above as max harvest amplitude m = 0,53·$W_{max}$. $W_{max}$ is the so-called capacity (maximum population density of fresh matter FM). W(t) = sigmoidal growth curve W′(t) = first derivation, indication the maximal growth rate at tp W‘‘(t) = second derivation, extrema indicating the max. harvest amplitude of the quasi linear growth zone in the middle of W(t) W’’’(t) = third derivation, more precise definition of the limits of the max. harvest amplitude as zero crossing of the function. Here as 0,53·W max.

A full-scale curve sketching is now possible in order to analyze the growth system as such already before modelling. The analytical result of the (non-numeric) equation Eq. (1) is that the term $W_{max}/2$ (half the capacity) occurs two times, firstly, as a multiplication factor before the functional, and secondly, in the argument of the tangens hyperbolicus function (see equation 2). This indicates that the real turning point **tp** of the sigmoidal function is the point of the maximum growth rate. This means that if conditions are kept at the optimum, such as temperature, light quality and quantity, the maximum possible harvest amplitude would be ≤53% of $W_{max}$ (variety-specific maximum capacity of the population).

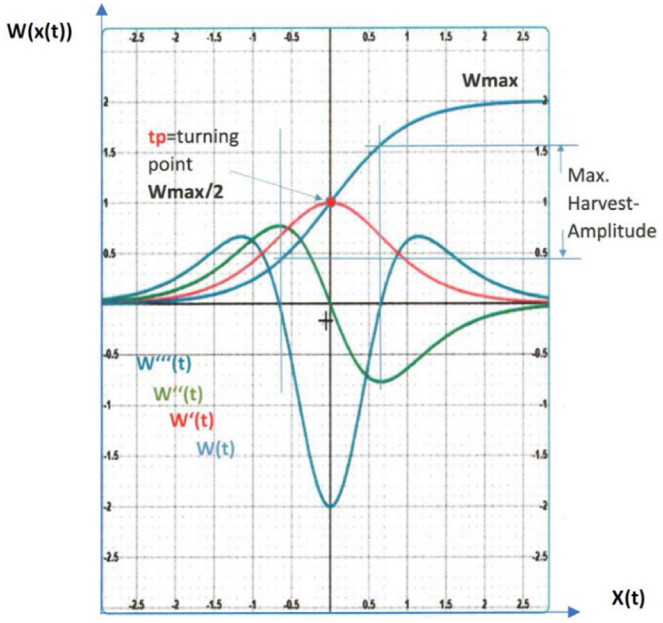


**Figure 3.** Curve delineating the differential equation Eq. (1) indicated above. The sigmoidal curve of limited growth is point symmetric around tp, which is the turning point. First derivation W′(t) indicated tp as the point of the maximum gradient (growth rate), which shows that tp = $W_{max}/2$.

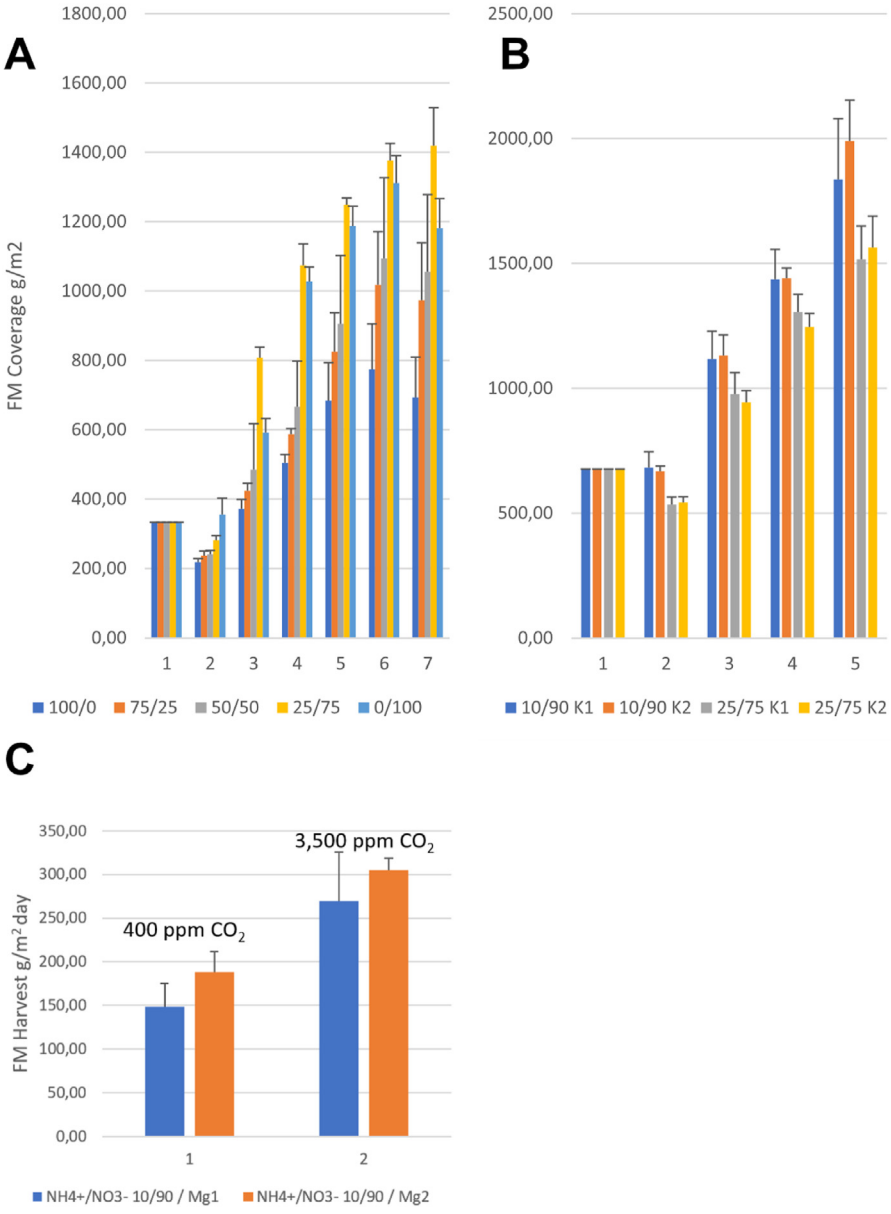


**Figure 4.** (**A**) Development of FM-coverage in $g \cdot m^{-2}$ at different $NH_4^+/NO_3^-$ ratios and a concentration of total N = 1.14 mM. Starting at a coverage of 333 g $m^{-2}$ the growth develops differently between the different $NH_4^+/NO_3^-$ -ratios. The coverage was measured every 3 days between the first and the seventh measurement. Figure 4(**B**) shows the growth with a further refinement of the $NH_4^+/NO_3^-$ ratio to 10/90 and added $CO_2$ at 3,500 ppm. Figure 4(**C**) shows the influence of a higher $CO_2$ concentration of 3,500 ppm compared to 400 ppm.

### 2.3.4. *Numeric programming of the model*

The model was programmed using SIMILE®, https://www.simulistics.com/, where numeric integration allows to test the influence of input parameters on growth. For a continuous culture, harvest intervals need to be optimized to assure a continuous biomass formation and to suppress algal growth. Thus, the harvest has to be carried out around the maximum growth rate, i.e. at the turning point of the growth function. This parameter had to be verified experimentally.

The harvesting amplitude (amount of partially harvested biomass FM) was chosen at around $W_{max}/2$ of the growth curve. The upper harvest point has to remain still at the quasi-linear gradient of the growth rate, which is ≤53% of $W_{max}$ like shown in Figure 3, and the harvest cycle has to be located symmetrically around the turning point tp. Thus, a factor m has to be implemented into the programming of SIMILE® within this analytically determined harvest amplitude: m ≤ 0.53. In order to be symmetrical around tp = $W_{max}/2$, the harvesting amplitude (amount of partially harvested biomass FM) can thus be described as:

$$|W_{\text{harvest}}| = \frac{Wmax}{2} * ((1 + m/2) - (1 - m/2)) \qquad \text{eq.11}$$

Since the harvest amplitude is m, and needs to be placed symmetrically around the turning point tp, it results in m/2 above and m/2 below tp. Harvesting thus starts at W1 as the upper point within the quasi-linear portion of the growth curve, which is

$$W1 = \frac{Wmax}{2} * (1 + m/2) \qquad \text{eq. 12}$$

and ends at the lower point, which is the remaining biomass after harvesting.

$$W2 = \frac{Wmax}{2} * (1 - m/2) \qquad \text{eq. 13}$$

Modelling for a further prediction is impossible without previously determining these parameters experimentally as the maximum biomass production differs widely between different genera and varieties or local races of *Lemnoideae*. The maximum biomass production per unit of area can be assessed once there is an equilibrium between growth and decay of fronds as shown below in Figures 5, 6, and 7. The results of the modelling are highly accurate and do coincide well with the measured data.

Assuming the growth rate within the complete harvesting amplitude as linear is an over-simplification. It would lead to erroneous results when running the model for long culture periods. The model has to calculate the growth function as well as the regrowth function after each harvest as a sigmoidal growth. The growth rate $r_i$, is only maximal at the turning point "tp" and assumed to be *quasi*-linear within the above-mentioned amplitude m. In contrast, the mathematically continuous sigmoidal curve will change through the harvesting process into a discontinuous delta function (sawtooth function). The numeric programming in SIMILE® was based on

$$\mathrm{dWgrowth} = \mathrm{ri}^{*}\mathrm{W(t)}\left(1 - \frac{\mathrm{W(t)}}{\mathrm{Wmax}}\right)^{*}\mathrm{dt}$$

as the operator for the numeric integration of limited growth. The operator $r_i$ was considered as a subroutine, or predetermined separately for $T$ (temperature) and $E$ (photoperiod), with the macro-nutrients N, P and $CO_2$, considered as pre-factors $\alpha, \beta, \gamma, \delta$ in the effective growth rate $ri$,

$$ri = ri0\left(\prod_{j=T,E,NP,CO2} k(ri(j))\right)$$

with $k = \alpha, \beta, \gamma, \delta$, with use of the predetermined values for *ri(T), ri(E), ri(N,P), ri($CO_2$),*

In order to implement the cyclic harvesting method additionally into the sigmoidal growth curve, resulting in a sawtooth shaped curve, the following codes can be directly introduced into the SIMILE® program with the following further operators for cyclic harvesting:

*$dW_{cyclic\ harvest}$ = if (W > W_$E_{cycL}$) then (W–W_$E_{Min}$)/dt() else 0.*

A further operator for the generation of fractals as a repeated loop for the harvesting impact is:

*$dW_{harvest}$ = if (Ist_harvest = = 1) then (W*m)/dt() else 0,*for regrowth and the next cyclic harvest.

## 3. Results

### 3.1. Optimization of the nutrient solution before modelling

First of all, the nutrient solution had to be optimized, as shown in Figure 4(**A**), for the $NH_4^+/NO_3^-$ ratios. The authors tested the ratios 100/0, 75/25, 50/50, 25/75, 0/100, grown to a population density of 1,419 g $m^{-2}$ FM. With a further refinement of the $NH_4^+/NO_3^-$ ratio to 10/90, as

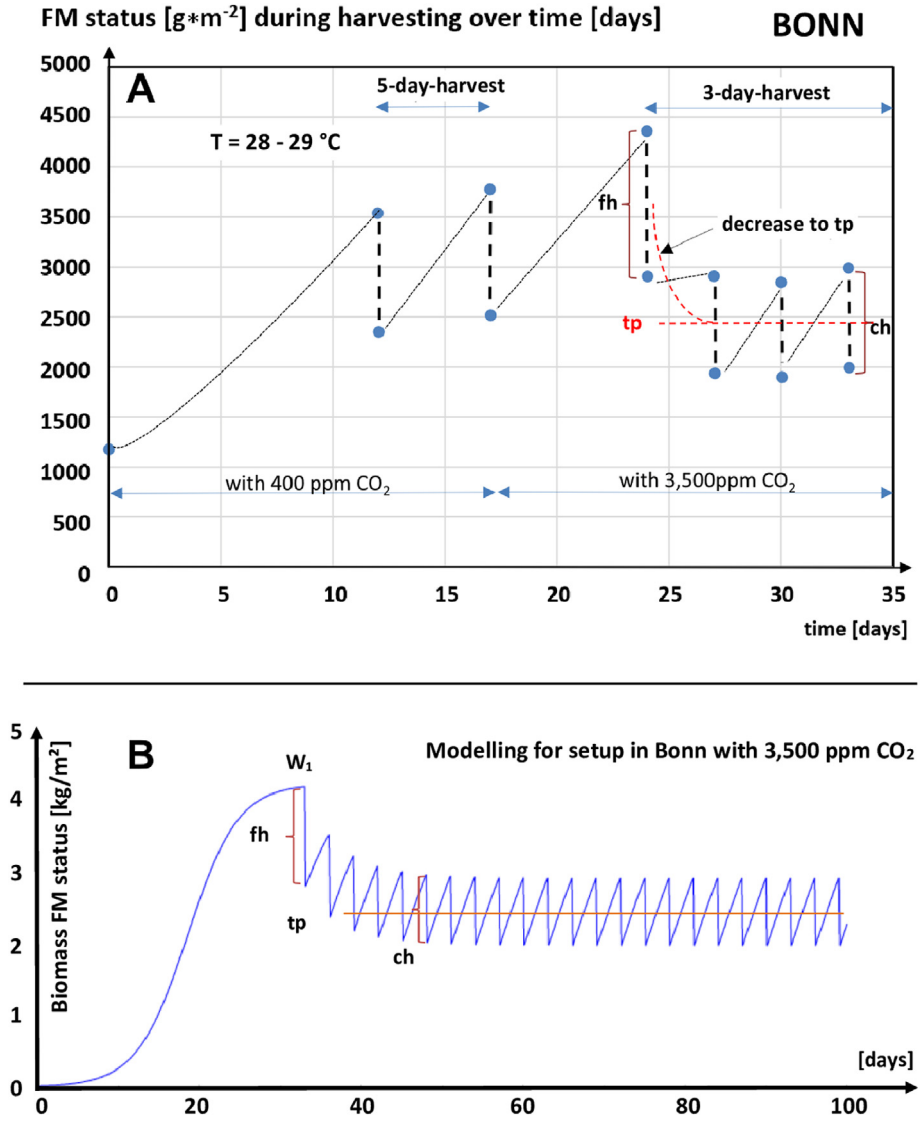


**Figure 5.** (**A**), FM biomass coverage resulting from the subsequent partial and cyclic harvesting. In the first part of the experiment the culture was operated at 400 ppm $CO_2$ for two harvests after 5 days each. When supplementing $CO_2$ at 3,500 ppm (v/v), the harvest interval was shortened from 5 to 3 days because of the higher growth rate. Figure 5(**B**) shows the related model run for 3,500 ppm $CO_2$ and harvesting intervals of 3 d.

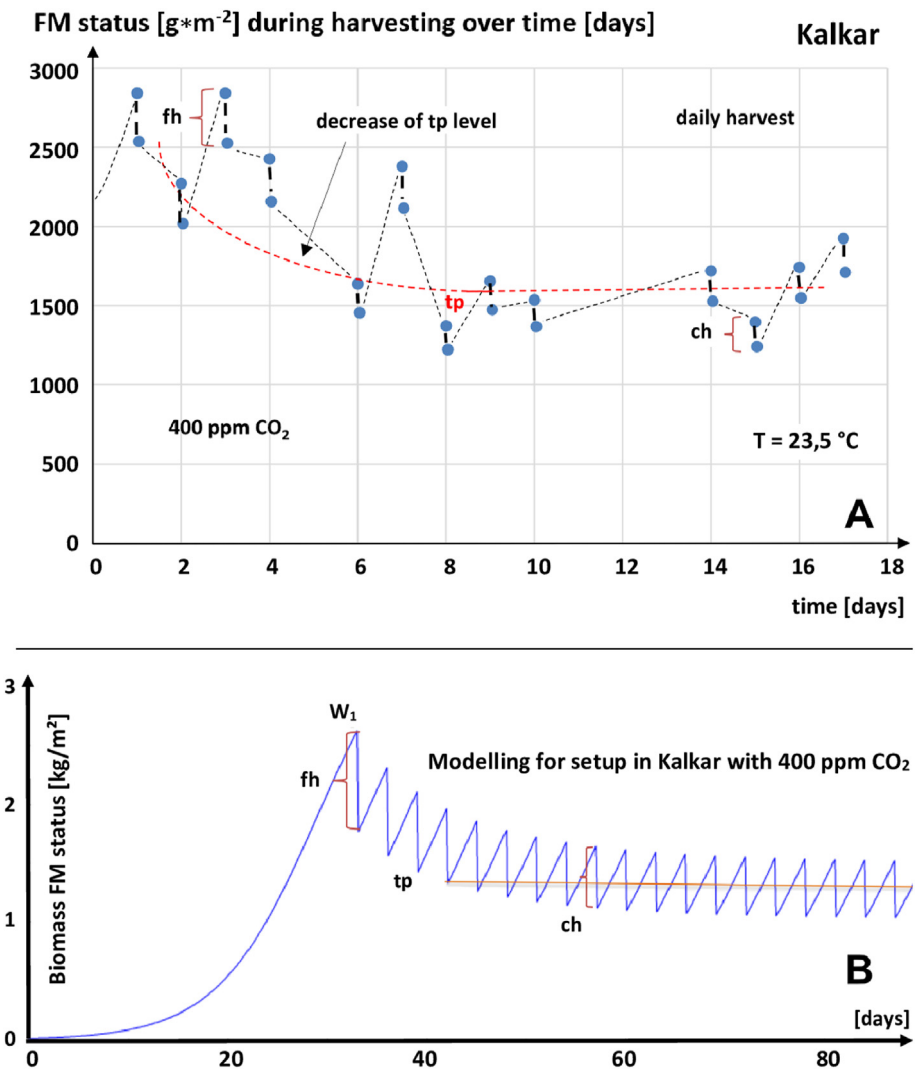


**Figure 6.** (**A**), FM yields during periodic harvest at the setup in Kalkar. It can be seen, that an upscaled system as such follows the same predictions from the modelling but with higher variations, which are caused by the much longer culture trays of 27m. In such long trays, the adequate expansion of the culture after partial harvesting is much more complicated as in shorter trays. The modelling in Figure 6(**B**) shows as well that the real data follow the prediction of the model.

shown in Figure 4(**B**), the culture grew to a coverage with a higher biomass density of 1,991 g $m^{-2}$ FM, (Figure 4(**A**) and 4(**B**)).

Figure 4(**A**) shows FM biomass growth with various $NH_4^+/NO_3^-$ -ratios measured every 3 days (72h). Point 1 is the starting biomass density. The experiment was run for 18 days. The $NH_4^+/NO_3^-$ -ratios used in the experiment were 100/0, 75/25, 50/50, 25/75, 0/100, with 4 replicates each. Figure 4(**A**) and 4(**B**) show the development of the FM coverage per tray indicated as g·$m^{-2}$. In a first approach, a $NH_4^+/NO_3^-$ -ratio of 25/75 yielded the best biomass production from the beginning and resulted in the highest coverage status of 1,419 g $m^{-2}$ with 400 ppm $CO_2$ and at 29 °C. With a further refinement (Figure 4(**B**), $NH_4^+/NO_3^-$ ratios of 10/90 resulted in the highest biomass production, confirmed further by yielding the lowest standard deviation.

According to Figure 4(**B**), we tested different N/K ratios (N/K1 = 1,07 and N/K2 = 0,83) in the same experiment, and reached a higher growth rate at N/K2. All other nutrients were supplied at concentrations high enough to avoid undersupply. Further values supporting this are shown in Figure 4(**C**), comparing biomass formation with and without additional $CO_2$ supply at two Mg concentrations of 0.2 and 0.4 mM. Optimum harvest was reached at 0.4 mM Mg, wherein the contribution by $CO_2$ at 3,500 ppm increased the biomass yield significantly. Again, $NH_4^+/NO_3^-$ = 10/90 resulted in the highest yields. The difference of maximum growth for 400 ppm and 3,500 ppm at $NH_4^+/NO_3^-$ = 10/90 is shown in detail in Figure 5. The N, P, K and Mg concentrations resulting as optimum in our experiments match literature values from Lasfar et al. (2007) and Cornish-Bowden (2015). For all subsequent experiments, the authors used $N_{total}$ concentrations of 1.14 mM, P at 0.23 mM, with a N/P ratio 5/1. These values are used in Eq. (7) below and also for the final experiments. The optimal temperature was 29 °C, as already shown by Landolt, Kandelar (1987) and Lasfar et al. (2007), and at 129μMol·$s^{-1}$·$m^{-2}$ PAR illumination, 90% of the maximum achievable growth rate was obtained.

### 3.2. Considering optimized parameters in the model

According to equations Eqs. (5), (6), (7), and (8), the k-factors for the specific growth rate are shown at the different experimental setups in the following overview. Once the effective tp was reached after several consecutive harvests it remained constant, even when starting at a higher coverage. This is due to the maximum regrowth rate around tp as shown in Figure 3.

The fresh matter (FM) growth rates *ri* resulting from Eq. (8) are compared in Table 1. The product of the co-factors $\alpha$, $\beta$, $\gamma$, *and* $\delta$ is termed "productivity factor". As a further test of plausibility, the column on the right-hand side shows the result assuming a maximum achievable growth rate $ri_{max}$ when setting the pre-factor product in Eq. (8) close to 1.

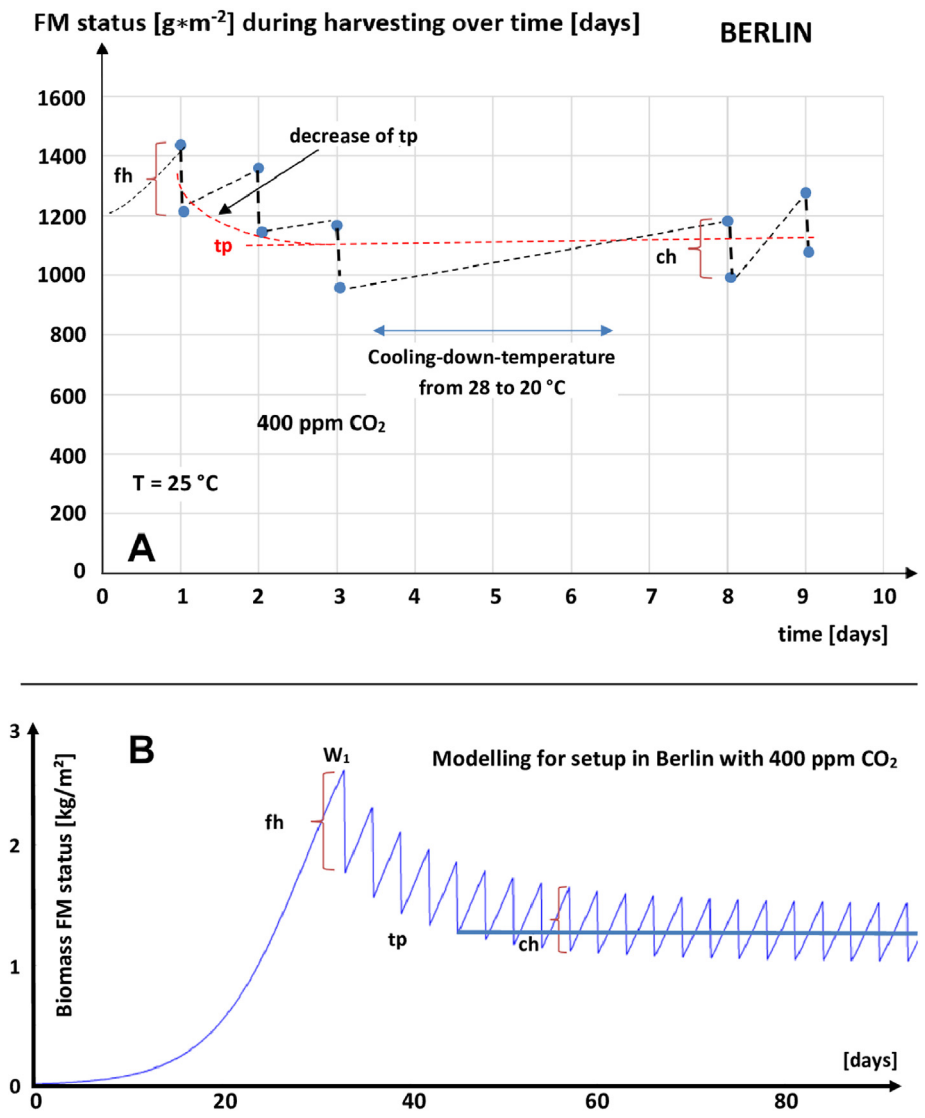


**Figure 7.** (**A**) Biomass harvested at the upskaled setup in Berlin with a rack system of 20m$^2$ aquatic culture surface. Figure 7(**B**) shows the related modelling which predicts the same effect as found in the measured data.

### *3.3. Comparison of data from experimental setups to modelled results*

The difference of the results represents the different SD (standard deviations) resulting from the different experimental settings (*$CO_2$ = 400 ppm, **$CO_2$ = 3,500ppm). According to the different conditions at the different experimental sites, the growth rate ri (in g FM·m$^{-2}$·d$^{-1}$) for Bonn ri = 216, for Kalkar 173 and for Berlin 190, with a capacity $W_{max}$ (in kg·m$^{-2}$ FM) of 3.80 at each experimental site. Initial biomass (g·m$^{-2}$) was 495 for Bonn, 450 for Kalkar and 500 for Berlin. Only in Bonn, additional $CO_2$ could be introduced (3,500 ppm), which resulted in a significantly higher growth rate ri of 323 (g·m$^{-2}$·d$^{-1}$) and a maximum capacity of 4.20 (kg·m$^{-2}$). All these starting values were fed into the model. The optimum nutrient solution as well as the N/P-depending term in the model (eq. 7) was based on $N_{total}$ = 1.14mM, $NH_4^+/NO_3$ 1/9, N/P = 5/1, N/K = 2/1, N/Mg = 10/1, with an accuracy of +/- 0.2μM. Figures 5, 6, and 7 show a specific effect, as predicted from the model: if the harvest starts at an already high biomass density (i.e. well above the tp), growth rates are declining quickly after the first harvest. Thus, the starting point W1 (see eq. 12) is far above the maximum growth rate, as can be seen from the growth curve in Figure 3. When keeping harvest intervals constant, the system will equilibrate towards a lower value. This model prediction was verified by real data as shown below. The authors suggest to term this effect "dynamic pinning" of the population towards the tp-point of the growth curve, i.e. at the maximum growth rate. This is valid if the intervals for the cyclic partial harvesting remain constant at three days. The **f**irst **h**arvest amounts in the model curves Figures 5(B),

**Table 1.** Calculated k factors: = α, β, γ, δ, considering the different conditions at the different setup locations and the belonging productivity factor $\prod_{j=T,E,NP,CO2} \boldsymbol{k}(\boldsymbol{ri}(j))$ using Eq. (8). (*$CO_2$ = 400 ppm, **$CO_2$ = 3,500ppm).

| | $\lvert\boldsymbol{\alpha}(\boldsymbol{ri}(\boldsymbol{T}))\rvert$ | $\lvert\boldsymbol{\beta}(\boldsymbol{ri}(\boldsymbol{E}))\rvert$ | $\lvert\boldsymbol{\gamma}(\boldsymbol{ri}(\boldsymbol{N},\boldsymbol{P}))\rvert$ | $\lvert\boldsymbol{\delta}(\boldsymbol{ri}(\boldsymbol{CO2}))\rvert$ | Productivity factor pf | Measured ri (average) [g FM·m$^{-2}$·d$^{-1}$] | Theoretical $ri_{max}$ = ri/pf [g FM·m$^{-2}$·d$^{-1}$] |
|---|---|---|---|---|---|---|---|
| Bonn** | 0.95 | 0.98 | 0.98 | 0.95 | 0.87 | 323 | 371 |
| Kalkar* | 0.85 | 0.98 | 0.90 | 0.69 | 0.52 | 173 | 332 |
| Berlin* | 0.89 | 0.98 | 0.95 | 0.69 | 0.57 | 190 | 333 |

6(B) and 7(B) are displayed as (kg FM·m$^{-2}$) and marked as **fh**. After equilibrating to a lower level symmetrically around tp, the harvest amplitude reduces to a **c**onsolidated **h**arvest amount (kg FM·m$^{-2}$) and is termed **ch**.

It can be seen that the starting point W1, defined by Eq. (12), reached a higher starting coverage with supplemental $CO_2$. The harvested biomass was reduced from first harvest (fh) equilibrated later on at a lower biomass production (consolidated harvest ch). When harvesting at the stage of the highest growth rate (tp) at a lower biomass (FM) status but with highest growth rate (tp), the model predicted the highest productivity which was confirmed by experimental data. This effect becomes visible when harvesting constantly every three days at the same interval, daytime and the same fraction from the maturation zone.

If the starting point $W_1$ is not located within the nearly linear range of the sigmoidal growth curve and if it is not symmetrical around the turning point tp, (Figures 3 and 5(**A**), 6(**A**), 7(**A**)), the productivity of the system declines until finally reaching a new equilibrium around the point of the highest growth rate = turning point (tp) of the sigmoidal growth function. With a decrease of the FM coverage, the possible production rate equilibrates from a first higher biomass fh (first harvest) to the consolidated harvest (ch). From that time on, the resulting constant harvest amplitude (ch) relates exactly to Eq. (11), including eq. 12 and eq. 13. In Figure 5(**A**) the experiment started with 5 days periodic harvesting at 400 ppm $CO_2$. After changing to a three-day harvest interval at 3,500 ppm $CO_2$, the regrowth gradient increased such that the cyclic harvesting time interval could be reduced from 5 to 3 days. The higher yield with higher $CO_2$ concentrations is verified and in line with the model prediction with the higher factor δ for $\delta \cdot ri_0(CO_2)$ (see eq. 9). Within the 5-day harvesting cycle, the starting point for harvesting matches perfectly. Within the 3-day harvesting cycle (with 3,500 ppm $CO_2$) the harvest starting point $W_1$ is out of range, so that the biomass is reduced from the first harvest (fh) to ch (consolidated harvest) amount as predicted. In Figure 5(**B**) the model results are compared to the measured curve in Figure 5(**A**), introducing the respective values for Wmax and ri into the modelling. The model curve shows the predicted values for 3,500 ppm $CO_2$. The modelled values coincide with the measured data. The ratios ch/fh between prediction (0.65) and measurement (0.67) match closely and are located within the range of the standard error. In the upscaled setups at Kalkar and Berlin, daily 1/3 of the maturation zone was harvested. Considering the propagation zone, this is 1/9 of the complete culture tray. Thus far, the conditions remained within the quasi-linear range around the turning point of the sigmoidal curve, harvesting 1/9 per day corresponds to 1/3 per 3-day harvesting. The model yields comparable data for the upscaled setups at Kalkar and Berlin.

According to Figure 6(**A**), the system behaves less predictable with high variations in the resulting harvest amplitudes, but over a longer period of time it follows the model prediction within the same trend. The dotted red line shows a smooth adaption to the "self centering" (pinning) value of maximal possible regrowth towards tp. In this setup, 1/3 of the culture surface of the LED-illuminated maturation zones was harvested. The maturation zone recovers by the extension of the biomass cover within this zone as well as by the expansion of the *Lemna* biomass from the propagation zone. Thus, the former gap was refed with new fronds from the complete culture surface. It can be seen in Figure 6(**A**), that in case of suboptimal conditions, e.g. suboptimum temperature, the growth rate $r_i$ is lowered. It shows as well, that the tp value is lower, which as well reduced the maximum capacity Wmax. Under those conditions, the regrowth of the culture system equilibrates at a lower level.

Very similar results were obtained for the set up at Berlin (Figure 7(**A**), 7(**B**)).

The same effect resulted in the set-up at Berlin under the same conditions as in Kalkar. The harvesting interval perfectly matches the harvesting time cycle when compared to the associated modelling in Figure 7(**B**). $CO_2$ increased the biomass formation (steeper gradient) and resulted in a higher tp point.

As could be seen and as predicted by the model (Figure 5(**B**)) for the laboratory set up in Bonn, the repeated harvesting described by the "sawtooth" curve leads to a lower equilibrium point (tp), because the harvesting cycle time was reduced from 5 to 3 days. The yield per harvest was reduced from 1080 g m$^{-2}$ for 5 days to 933 g m$^{-2}$ for 3 days harvest periods; i.e., recalculated on the base of FM in g per m$^2$ and day from 216 g d$^{-1}$ m$^{-2}$ to 313 g d$^{-1}$ m$^{-2}$, this results in a yield increase of 44% per day by $CO_2$ at 3,500 ppm. The effects of variations in nutrient supply, temperature, (Bernacchi et al., 2002), light spectral composition, and $CO_2$ supplement can thus be predicted.

The differences in biomass yield between laboratory set up and upscaled set up can be explained by the lower cultivation temperature, (5.5 K lower) and without added $CO_2$, compared to the constant optimum of 29 °C at Bonn. Biomass yield was reduced by a factor $ri(T) < 1$ (in eq. 8) with -3% per °C between 21 and 29 °C, with a longterm average of 23.5 °C. This is 5.5 K lower as the optimum 29 °C. Thus, the temperature related factor of the growth-rate can be calculated as α(ri(T))-factor, which is of $1/1.03^{5,5} = 0.85$ according to Eq. (8).

### 3.4. Accuracy of predicted dynamic effects compared to real data

Figures 5, 6, and 7 compare the results from measurement to the modelling. Starting at a coverage density beyond the quasi-linear exponential growth range, limited by the curve sketching in Figure 4, the sawtooth function equilibrates at a value where it is centered symmetrically around the maximum regrowth gradient at tp, the point of maximum growth rate. The experimental data fully confirm the model predictions qualitatively and quantitatively.

Table 2 shows the accuracy between model calculations and real measurements. The declining biomass yield, starting from a higher biomass coverage and equilibrating around tp was precisely predicted by the model. This agrees with all measurements at each location and all experimental setups. The setup in Bonn supports the cultivation and cyclic harvesting with the optimum conditions for growth. Thus, the model matches the measurements to 101%. The setups in Kalkar and Berlin still match the model prediction with 74% and 78 % rather well, considering that the conditions could not be controlled as precisely as in the lab system and that there were sometimes suboptimum conditions in the larger scale systems.

## 4. Discussion

### 4.1. Optimized nutrient solution for long-term cultivation

*Lemna* spp. are mostly indicators for higher nitrate levels in water bodies and nitrate is their preferred N form. Similar to other low-light tolerant and/or short days species, nitrate serves *i.a.* as osmoticum for growth. Thus, those species usually are less tolerant against higher ammonium levels (Quingyang Zhou et al., 2017; Bloom-Zandstra, Lampe, 1985).

In our experiments, a ratio of 1/9 $NH_4^+/NO_3^-$ resulted in the highest constant growth rates and kept pH values constant over an extended period, balancing proton consuming and proton releasing processes.

**Table 2.** Comparison of FM (Fresh matter) first harvest **fh** and consolidated harvest **ch** between modelling and measure.

| | fh (mod) kg FMm$^{-2}$ d$^{-1}$ | ch (mod) kg FMm$^{-2}$ d-1 | ch/fh (mod) | ch/fh (measure) | Accuracy (mod/meas) |
|---|---|---|---|---|---|
| BONN** | 0.450 | 0.313 | 0.673 | 0.667 | 101% |
| KALKAR* | 0.305 | 0.173 | 0.567 | 0.767 | 74% |
| BERLIN* | 0.286 | 0.190 | 0.664 | 0.848 | 78% |

** 3,500 ppm $CO_2$,
* 400 ppm $CO_2$.

Khvatkov et al. (2019) found 1/13 as optimum $NH_4^+/NO_3^-$ ratio, however under axenic conditions and at half the PAR, whereas Petersen et al. (2021) identified 25/75 as optimum, but only for one harvest under short-term cultivation.

It has to be seen that any factor hampering with the *Lemna* growth will result in algae outgrowing the duckweed (Szabo et al., 2005). Even though $NH_4^+$ uptake rates are usually higher for many plants, $NO_3^-$ is the preferred form in *Lemna* spp. This may be due to the fact that *Lemna minor* as low light tolerant species uses nitrate as an osmoticum, similar to e. g. nitrate in osmoregulation of lettuce or spinach grown at lower light intensities (Blom-Zandstra, Lampe 1985). Furthermore Ferreira, Shaw (1989) could verify that although many proteins from the fronds of *Lemna minor* undergo enhanced degradation during osmotic stress, ribulose-1,5-biphosphate carboxylase (RuBPCase) is not degraded. This provides further evidence that nitrate as osmoticum is relevant for *Lemna* species as well, especially under low light conditions. In addition, a higher $NH_4^+$ concentration means a higher proton input, acidification of the cytoplasm and strong C drain of oxoglutarate from the TCC (Marschner's textbook, Marschner et al., 2012)

Besides the ratio of $NH_4^+/NO_3^-$, the total N supply is one main driver for growth. Here again, an oversupply may favour algal development whereas undersupply would not allow to exploit the full potential of *Lemna* as the fastest growing Angiosperm (Ziegler et al., 2015). The best concentration for total N in our experiments was 1.14 mM, a value lower than reported by Petersen et al. (2020) and Khvatkov et al. (2019). The authors based their nutrient supply on the concentrations found in the young (high quality) plant material and the growth rates found in many previous experiments. Thus, the nutrient supply was designed to meet the *Lemna* crop's requirements, avoiding both over-as well as undersupply. In addition, as nutrients were almost continuously re-supplied a lower "nutrient buffer" is needed compared to frequently used setups with a static culture. In order to prevent an unwanted nitrate accumulation in the biomass, as observed by Devlamynck et al. (2020) at higher nitrate concentrations, the authors recommend to keep the total N-concentration in the nutrient solution at the aforementioned lower level of 1.14 mM, refeeding N twice or thrice a day to balance the concentration with the actual consumption.

Concentrations of K in our experiments were kept lower than in the above cited approaches, likewise avoiding the buildup of unused nutrients in the nutrient solution. Mg supply was identified as critical as well with an optimum around 0,4 mM. The effect was especially prominent with an increase by almost two thirds when raising $CO_2$ levels to 3,500 ppm.

The authors could verify that comparable biomass yields can be obtained at different experimental scales from the 0.018 $m^2$ at Bonn through $20m^2$–$300m^2$ of aquatic surface in the other premises. Nevertheless, the laboratory results are close to the modelling with an accuracy of 99% related to the model predictions, whereas the upscaled set-ups in Kalkar and Berlin coincided by only 74% and 78 %. The reason is that refeeding the nutrients was carried out once a day, sometimes even every two days. Furthermore, temperature could not be controlled as precisely as in the lab approach. It was also shown that decreasing values for T and $CO_2$ lead to a decreasing yield, as shown in Figure5, 6, and 7.

To obtain higher growth rates in the larger production systems, a constant nutrient supply just compensating the uptake by the biomass is required.

### 4.2. Light and temperature conditions

Supplemental light intensity was lower in our approaches than the PAR provided by Petersen et al. (2021). Considering, though, that these authors provided only 8 h per day of light, while in our approach all experiments were kept at 16 h light and 8h dark. In sum, the integral of light supply over time was comparable in both approaches, but the higher day length has the added advantage of a longer period for photosynthesis and a shorter period of respirational losses. The temperature in our lab experiments was 29 °C and coincides with the optimum temperatures as determined by Lasfar et al. (2017).

### 4.3. Model approach

Khvatkov et al. (2019) focused his model basically on nutrient ratios, developed by the evaluation of biomass yields in an MS-Excel based calculation.

In the so called ECOFERM project in Netherlands 2016, several modelling approaches for determining growth-rates in upscaled culture systems from de Wilt et al. (2016), Lasfar et al. (2007) and from Goudriaan, van Laar (1985) were used to predict the growth of *Lemna* in indoor ponds. Deviations of about 100% and more were found between measured data and modelling. Since Driver et al. (2005) it is well known that the growth of *Lemna minor* is limited when reaching high plant densities in the culture. Thus, the growth has to be described by the differential equation for limited growth and it yielded the best fit between modelled and measured data. In contrast to van Dyck et al. (2022), the deviation of biomass prediction between model and laboratory set-up in this work is only about 1%. Reason for this is the precise adjustability of the optimal parameters in the laboratory scale. Furthermore, the dependencies of the growth rate *ri* to temperature, light (quantity and quality), macronutrient ratios and additionally $CO_2$ were considered conclusively and not separately. By the updated approach of Liebig's law of the minimum along the product rule, the modelling as such includes all relevant variables in one final step.The introduction of a discontinuous sawtooth curve for periodic partial harvesting into the analytical sigmoidal growth curve, describing the regrowth, resulted in an evidently better accuracy between experiments and model results. In contrast to van Dyck et al. (2022), Petersen et al. (2022), and Khvatkov et al. (2017), the authors in this work provide a modelling that not only describes one sigmoidal growth, but also models sustainable cyclical harvesting dynamics of the population. So the possible maximum growth rate *ri* of FM of about 323 $gm^{-2}d^{-1}$ can be reached as possible maximum at 3,500 ppm in a sustainable way in an upscaled production system. Thus, it could be shown that the parameters have to be kept as near as possible to their respective optima. One has to keep in mind, that a high growth rate is required to suppress competing algal growth. Thus, the harvest schedules have to be kept as well at a rate where *Lemna* growth rates are as high as possible to successfully compete with algal growth.

So the authors model predicted a regular sawtooth curve along which regular partial harvesting around maximum growth rate obtain the maximum biomass yield over time. The calculations show as well that the balance between uptake and resupply of nutrients at a low N-level, keeping the nutrient ratios as shown above, results in a constant pH of about 6.5, which as well lowers the chance of competing algal growth. This eliminates the need for all other algae co-population suppression measures.

## 5. Conclusions

The aim of the work was to optimize growth parameters for a continuous year-round large scale *Lemna* production under non-sterile conditions in greenhouses, with respect to nutrient and $CO_2$ supply, additional lighting, and harvest intervals. Besides the productivity, one of the challenges is to avoid competing algal growth in the cultures.

When optimizing the nutrient supply, we parted from the need to keep pH and N supply rather constant at an optimum level for *Lemna* growth. To keep the cultures in the slightly acidic pH range, the optimum $NH_4^+/NO_3^-$ ratio was found to be 1:9 at a total N-level of 1.14 mM. Higher concentrations would favour competing algal growth, lower values result in delayed *Lemna* development and reduced surface coverage. Best results were obtained with a modified Hoagland solution as indicated in materials and methods. Given the multitude of possible combinations, a model was developed to assess the influence of culture parameters including light, supplemental $CO_2$ and harvest intervals and fractions of

the total biomass. In many publications, parameters were only assessed for short – term (e.g. 7 day) growth periods, which however is way too short to assess the optimum settings for a continuous year-round production. As harvesting schedules were found to be decisive for a stable culture, harvesting one third of the biomass every 5 days at 400ppm $CO_2$ and every 3 days at 3,500ppm $CO_2$ resulted as optimum. This allows FM harvests of 323 g $m^{-2}$·$d^{-1}$, i.e. almost 120 kg FM·$m^{-2}$ per year at 3,500 ppm $CO_2$. Model data were validated with existing systems from lab to greenhouse scale and confirm the relevance of choosing the proper harvest intervals.

As *Lemniodeae* are heavy metal hyperaccumulators (Khellaf, Zerdoani, 2009; Kamal et al., 2004) trace element supply, especially of Fe, Zn and Cu, has to be optimized to avoid an unwanted accumulation but to still allow high growth rates and optimum product quality. The continuous biomass harvesting (every 3 days) reduces the statistical age of the fronds from about 21 days to only 4–5 days and thus significantly reduces the chance for hyperaccumulation of heavy metals. Thus, the harvest intervals as found by the model approach maximizes biomass yield while reducing the risk of accumulation of heavy metals.

While the nutrient supply in our experiments was already close to optimum, there are still some parameters which could possibly be optimized such as micronutrient ratios, $CO_2$ concentrations and supplemental light in quality and quantity. The developed model will aid in setting the best parameter values and thus helps to optimize production parameters under different conditions. It can be fed into a computer-aided control system for automated indoor production of *Lemna spp.*. Further research will have to be directed at optimizing the system for defined qualities like protein contents or other valuable plant constituents (PUFA).

## Declarations

### *Author contribution statement*

Karl Michael Schmidt: Conceived and designed the experiments; Performed the experiments; Analyzed and interpreted the data; Contributed reagents, materials, analysis tools or data; Wrote the paper.

Heiner Goldbach: Analyzed and interpreted the data; Contributed reagents, materials, analysis tools or data; Wrote the paper.

### *Data availability statement*

Data will be made available on request.

### *Declaration of interests statement*

The authors declare no conflict of interest.

### *Additional information*

No additional information is available for this paper.

## References


Acosta, K., Appenroth, K.J., Borisjuk, L., Edelman, M., Heinig, U., Jansen, M.A.K., Oyama, T., Pasaribu, B., Schubert, I., Sorrels, S., Sree, K.S., Xe, S., Todd, P.M., Lam, E., 2021. Return of the Lemnaceae: duckweed as model plant system in the genomics and postgenomics era. Plant Cell 33 (10), 3207–3234.

Appenroth, K.J., Sree, K.S., Bohm, V., Hammann, S., Vetter, W., Leiterer, M., Jahreis, G., 2017. Nutritional value of duckweeds (Lemnoideae) as human food. Food Chem. 217, 266–273.

Bloom-Zandstra, M., Lampe, E.M., 1985. The role nitrate in osmoregulation of lettuce (*Lactuca sativa* L.) grown at different light intensities. J. Exp. Bot. 36 (7), 1043–1052. July 1985.

Von Caemmerer, S., Farquhar, G.D., 1981. Some relationships between the biochemistry of photosynthesis and the gas exchange of leaves. Planta 153, 376–387, 1981.

Calabrese, M.G., Ferranti, P., 2019. New food sources. Encycl. Food Secur. Sustain. 1, 271–275.

Chakrabarty, R., Clark, W.D., Sharma, J.G., Goswami, R.K., Shrivastav, A.K., Tocher, D.R., 2018. Mass production of *Lemna minor* and its amino acid and fatty acid profiles. Front. Chem. 2018.

Cornish-Bowden, A., 2015. One hundred years of Michaelis menten. Persp. Sci. 4, 3–9. March 2015.

Coughlan, N.E., Walsh, E., Bolger, P., Burnell, G., O Leary, N., O Mahoney, M., Paolacci, S., Wall, D., Jansen, M.A.K., 2022. Duckweed bioreactors: challenges and opportunities for large-scale indoor cultivation of Lemnaceae. J. Clean. Prod. 336, 130285.

Devlamynck, R., de Souza, M.F., Bog, M., Leenknegt, J., Eeckhout, M., Meers, E., 2020. Effect of the growth medium composition on nitrate accumulation in the novel protein crop *Lemna minor*. Ecotoxicol. Environ. Saf. 206, 111380, 2020.

Docauer, D.M., A Nutrient Basis for the Distribution of the Lemnaceae, University of MichiganProQuest Dissertations Publishing, Degree Year1983. 8324164, pp 34-46.

Driver, S.M., Nes, E.H.V., Roijackers, R.M., 2005. Growth limitation of *Lemna minor* due to high plant density. Aquat. Bot. 81, 245–251.

Van Dyck, I., Vanhoudt, N., Batlle, J.V., Hormans, N., Nauts, R., Van Gompel, A., Claesen, J., Vangronsveld, J., 2021. Effects of environmental parameters on *Lemna minor* growth: an integrated experimental and modelling approach. J. Environ. Manag. 300, 113705.

Evans, J.R., Kaldenhoff, R., Genty, B., Terashima, I., 2009. Resistance along the CO2 diffusion pathway inside leaves. J. Exp. Bot. 60 (8), 2235–2248.

Farquhar, G.D., von Caemmerer, S., 1982. Modelling of photosynthetic responses to environmental conditions. Physiol. Plant Ecol. Encycl. Plant Physiol. 12/B (920), 549–587.

Ferreira, R.B., Shaw, N.M., 1989. Effect of osmotic stress on protein turnover in *Lemna minor* fronds. Planta 179 (4), 456–465, 1989.

Goudriaan, J., van Laar, H.H., 1994. Modelling Potential Crop Growth Processes. Springer-Science + Business media B.V.

Hikosaka, K., Niinemets, U., Anten, N.P., 2015. Canopy Photosynthesis: from Basics to Applications. Springer, pp. 79–83.

Hoagland, D.R., Arnon, D.I., 1950. The Water-Culture Method for Growing Plants without Soil, 347. Circular/University of California, College of Agriculture, Agricultural Experiment Station, Berkeley, pp. 347–353. No 2nd edit.

Kamal, M., Ghaly, A.E., Mahmoud, N., Cote, R., 2004. Phytoaccumulation of heavy metals by aquatic plants. Environ. Int. 29, 1029–1039. https://doi.org/10.1016/S0160-4120(03)00091-6.

Khellaf, N., Zerdaoui, M., 2009. Growth response of duckweed *Lemna minor* to heavy metal pollution, Iran. J. Environ. Health Sci. Eng. 6 (3), 161–166.

Khvatkov, P., Chernobrovkina, M., Okuneva, A., Dolgov, S., 2019. Creation of culture media for efficient duckweeds micropropagation (*Wolffia arrhiza* and *Lemna minor*) using artificial mathematical optimization models. Plant Cell Tissue Organ Cult. 139.

Kuehdorf, K., Appenroth, K.J., 2012. Influence of salinity and high temperature on turion formation in the duckweed *Spirodela polyrhiza*. Aquat. Bot. 97 (1), 69–72. February 2012.

Landolt, E., Kandelar, R., 1987. Biosystematic Investigations in the Family of Duckweed (Lemnaceae). In: The Family of Lemnaceae – A Monographic Study, 4. Geobotanisches Institut ETH: Zürich, Germany, 1987.

Landolt, E., Luond, A., Kandeler, R., 1987. Biosystematic investigation in the family of duckweeds, Veröffentlichungen des Geobotanischen Instituts der ETH Zürich. Stiftung Ruebel; Heft 70 (71), 80–95.

Lasfar, S., Monette, F., Millette, L., Azzouz, A., 2007. Intrinsic growth rate: a new approach to evaluate the effects of temperature, photoperiod and phosphorus-nitrogen concentrations on duckweed growth under controlled eutrophication. Water Res. 41 (11), 2333–2340.

Litchman, E., 2007. Resource competition and the ecological success of phytoplankton. Evol. Prim. Prod. Sea 351–375. Academic Press.

Marschner, P., et al., 2012. Marschners Mineral Nutrition of Higher Plants. Elsevier Amsterdam, pp. 136–146.

Morris, S.J., Blackwood, C.B., 2017. The Ecology of Soil Organisms, Soil Microbiology, Ecology and Biochemistry, third ed., pp. 195–229

Petersen, F., Demann, J., Restemeyer, D.J., Ulbrich, A., Olfs, H.-W., Westendarp, H., Appenroth, K.-J., 2021. Influence of the nitrate-N to ammonium-N ratio on relative growth rate and crude protein content in the duckweeds *Lemna minor* and *Wolffiella hyalina*. Plants 10, 1741, 2021.

Petersen, F., Demann, J., Restemeyer, D., Olfs, H.W., Westendarp, H., Appenroth, K.J., Ulbrich, A., 2022. Influence of light intensity and spectrum on duckweed growth and proteins in a small-scale, re-circulating indoor vertical farm. Plants 11 (8), 1010.

Raven, J., Osborne, B., Johnston, A., 1985. Uptake of $CO_2$ by aquatic vegetation. Plant Cell Environ. 8 (6), 417–425.

Schmidt, K.M., 2020. Method for operating a culture facility for aquatic plants, and culture facility itself (DE 10 2020 133 132 A1). Deutsches Patent- und Markenamt. https://register.dpma.de/DPMAregister/pat/register?AKZ=1020201331320.

Schmidt, K.M., 2021. Method for Operating a Culture Facility for Aquatic Plants, and Culture Facility Itself (WO2022123076A1). European Patent Office. https://worldwide.espacenet.com/publicationDetails/originalDocument?FT=D&date=20220616&DB=&locale=en_EP&CC=WO&NR=2022123076A1&KC=A1&ND=4#, filed.

Schmidt, K.M., Rogmans, M., Wilhelm, H.J., 2018. Method for operating a culture system for protein-rich aquatic plants, as well as the culture system itself (DE 10 2018 003 368 B3). Deutsches Patent- und Markenamt. https://register.dpma.de/DPMAregister/pat/register?AKZ=1020180033687,granted.

Smith, V.H., Schindler, D.W., 2009. Eutrophication science: where do we go from here?, 24, pp. 201–207. Issue 4.

Soong, J.L., Fuchslueger, L., Marañon-Jimenez, S., Torn, M.S., Janssens, I.A., Penuelas, J., Richter, A., 2020. Microbial carbon limitation: the need for integrating microorganisms into our understanding of ecosystem carbon cycling, 26, pp. 1953–1961. Issue 4.

Stewart, J.J., Adams, W.W., Escobar, C.M., Lopez-Pozo, M., Demmig-Adams, B., 2020. Growth and essential carotinoid micronutrients in *Lemna gibba* as a function of growth light intensity. Front. Plant Sci. 11, 480.

Szabo, S., Roijackers, R., Scheffer, M., Borics, G., 2005. The Strength of limiting factors for duckweed during algal competition. Arch. Hydrobiol. 164 (1), 127–140.

Ueda, K., Nagai, T., 2021. Relative sensitivity of duckweed *Lemna minor* and six algae to seven herbicides. J. Pestic. Sci. 46 (3), 267–273.

Ueno, K., Ito, S., Oyama, T., 2021. An endogenous basis for synchronisation characteristics of the circadian rhythm in proliferating Lemna minor plants. New Phytol. Volume233 (Issue5), 2203–2215, 2022.

Warsi, O.M., Dykhuizen, D.E., 2017. Evolutionary implications of Liebig's law of the minimum: selection under low concentrations of two non-substitutable nutrients. Ecol. Evol. 5296–5309. Volume7, Issue14, 201.

Zhou, Quingyang, Gao, Jinqing, Zhang, Ruimin, Zhang, Ruiqin, 2017. Ammonia stress on nitrogen metabolism in tolerant aquatic plant *Myriophyllum aquaticum*. Ecotoxicol. Environ. Saf. 143, 102–110, 2017.

Ziegler, P., Adelmann, K., Zimmer, S., Schmidt, C., Appenroth, K., 2015. Relative *in vitro* growth rates of duckweeds (Lemnaceae) – the most rapidly growing higher plants. Plant Biol. 17, 33–41. open.efsa.europa.eu/. https://www.simulistics.com/. https://open.efsa.europa.eu/questions/EFSA-Q-2020-00512.